Proceedings of ASME Turbo Expo 2014: Turbine Technical Conference and Exposition
GT2014
June 16 – 20, 2014, Düsseldorf, Germany

GT2014-25570

The Design of a Steady Aero Thermal Research Turbine (START) for Studying Secondary Flow Leakages and Airfoil Heat Transfer

Michael Barringer, Andrew Coward, Ken Clark, and Karen A. Thole
Mechanical and Nuclear Engineering Department
The Pennsylvania State University
University Park, PA 16802

John Schmitz and Joel Wagner
United Technologies Corporation
Pratt & Whitney
East Hartford, CT 06108

Mary Anne Alvin, Patcharin Burke, and Rich Dennis
U.S. Department of Energy
National Energy Technology Laboratory
Pittsburgh, PA 15236

ABSTRACT

This paper describes a new gas turbine research facility that was designed and is currently being constructed with a number of unique features that allow experiments which aim at developing and improving sealing and cooling technologies at a reasonable cost. Experiments will include engine-representative rotating turbine hardware in a continuous, steady-state, high-pressure flow environment. The facility includes a 1.5 stage turbine that will simulate the aerodynamic flow and thermal field interactions in the engine between the hot mainstream gas path and the secondary air flows at relevant corrected operating conditions and scaling parameters. Testing in the new facility is planned to begin in 2014 and will take place in two phases. The first phase is focused on understanding the behavior of inner-stage gap flow leakages in the presence of the main gas path and the rotating blade platform. The second phase is focused on developing and testing novel cooling methods for turbine airfoils, platforms, and disks, ultimately leading to an integrated approach for more effective use of the secondary cooling flow. The uniqueness of this facility includes a continuous duration facility with engine-relevant rotational and axial Reynolds and Mach numbers at the blade inlet.

INTRODUCTION

One of the biggest challenges of today in the gas turbine engine industry is the recent increase in fuel costs that contribute substantially to end user operating budgets. It is imperative that gas turbine propulsion systems and land-based power generation systems become more fuel efficient. To this end, turbine designers and supporters are focusing on new engine architectures to achieve sustainable performance and efficiency goals. A recent goal set by the United States Department of Energy - National Energy Technology Laboratory (N.E.T.L.) is to increase the efficiency of land-based, combined-cycle, power plants by 3-5%. The efficiency increase will be achieved by reducing secondary air system flow leakages within the turbine section of the engine, thus reducing fuel burn, and by permitting higher turbine firing temperatures by using more advanced cooling designs.

Although engine architecture is a prime driver for performance enhancement of both aircraft and land-based turbines, cycle variations are also a major factor. Recent engine offerings indicate that engines with higher overall pressure ratio will be the norm rather than the exception. As a result, component cooling in the engine hot section is increasingly challenged with the need to cool parts with increasingly warmer cooling air. Moreover, cooling flow rates need to be reduced rather than increased as higher cooling temperatures would dictate to meet today's high-performance requirements. Future requirements of engine performance mandate a paradigm shift in the usage of secondary flow and cooling in the turbine. Nearly one quarter of the total air flow through a gas turbine engine bypasses the combustor and is used for cooling turbine airfoils, disks, and other turbine components, as shown in Figure 1. It is vital that new, low-flow cooling and aerodynamic technologies be developed to reduce the airfoil cooling and secondary air system flow rates while improving the effectiveness of available cooling flows.

By reducing the amount of turbine cooling air and eliminating unintended leakage paths, a reduction in the fuel burn can be achieved. Instead of wasting the valuable, high-pressure, secondary cooling flow, it can be used to further cool other turbine components using advanced cooling designs, thereby allowing higher firing temperatures, and thus higher engine efficiencies. A better understanding of how the individual leak paths affect one another and how they influence the overall performance of the turbine is needed to ensure that design requirements for turbine part life are met.

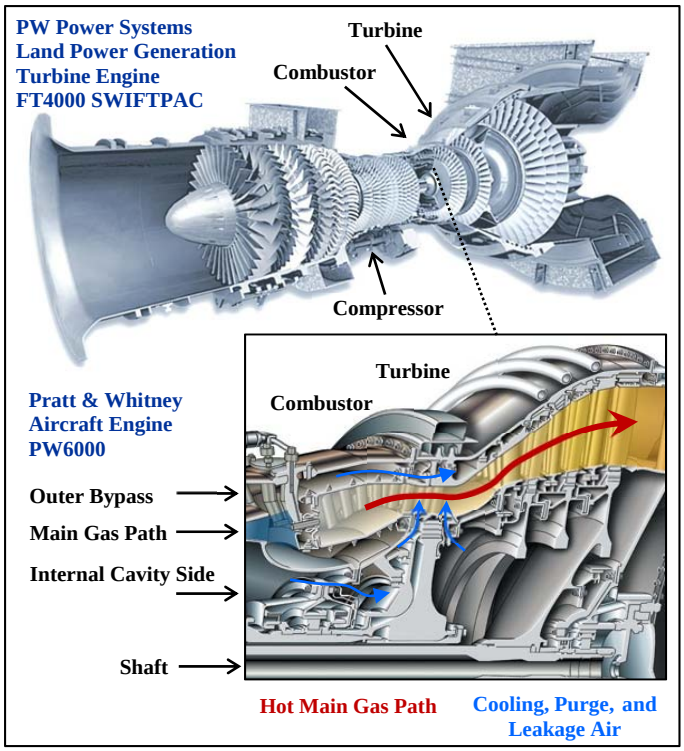

Figure 1. Example gas turbine engines from PW Power Systems and Pratt & Whitney highlighting the turbine hot main gas path and secondary cooling flow paths [1].

In this new facility, research is focused on addressing the fundamental flow effects of rotation on secondary air systems and aero-thermal cooling in a gas turbine. The goal is to demonstrate increased turbine efficiency by reducing cooling flow to the turbine through the systematic study of dedicated turbine cooling, purge, leakage, and primary core flow interactions. The new facility will be used to study the following five main topics: (1) the influence of leakage flows from the internal secondary air system on turbine stage aerodynamics and heat transfer, (2) disruptive new designs in sealing the interfaces between stationary and rotating components, (3) cooling flow performance inside and outside airfoils under rotation with secondary air system leakage, (4) the impact of separately optimized designs versus combined system optimization, and (5) hardware design for variation.

NOMENCLATURE

a vane or blade pitch
b hub radius, or disk radius at rim seal
C_p pressure coefficient, $C_p = \frac{P_{0,in}-P_{0,ex}}{P_{ref}}$
C_x axial chord
C_w nondimensional purge mass flow rate, $C_w = \frac{\dot{m}}{\mu_c b}$
$\dot{m}$ mass flow rate
p pressure, static pressure
r radius, radial direction
R gas constant
Re_x axial Reynolds number, $Re_x = \frac{\rho u_x C_x}{\mu}$
Re_ϕ rotational Reynolds number, $Re_\phi = \frac{\rho \Omega r^2}{\mu}\Big|_{hub,C}$
T temperature
U velocity
x axial direction
Zw Zweifel, $Zw = 2\frac{a}{C_x}\cos^2\beta_2(\tan\beta_1 + \tan\beta_2)$

Greek

β airfoil flow angle
γ ratio of specific heats
ε_c concentration effectiveness, $\varepsilon_c = 1 - \frac{C_{w,in}}{C_{w,eg}} = \frac{\chi - \chi_{mgp}}{\chi_p - \chi_{mgp}}$
η_{TT} total-to-total efficiency, $\eta = \frac{1-(T_{0,ex}/T_{0,in})}{1-(P_{0,ex}/P_{0,in})^{(\gamma-1)/\gamma}}$
η_τ torque-based efficiency, $\eta = \frac{\Omega\tau}{\dot{m}c_p T_{0,in}[1-(P_{0,ex}/P_{0,in})^{(\gamma-1)/\gamma}]}$
λ_T turbulent flow parameter, $\lambda_T = C_w Re_\phi^{-0.8}$
μ dynamic viscosity
ρ density
ϕ circumferential, tangential direction
Φ flow coefficient, $\Phi = \frac{u_{x,in}}{\Omega r}$
τ torque
χ gas concentration
Ω rotational speed

Subscripts

∞ freestream, or main gas path (mgp)
0 denotes stagnation property
1 1st vane inlet value
2 1st vane exit/rotor inlet value
C denotes coolant supply quantity
in denotes inlet value
ex denotes exit value
mgp main gas path
p purge cooling flow
ref reference
x axial direction

RELEVANT LITERATURE

The open literature contains numerous turbine rig facilities. Most of the studies from these facilities have focused on better understanding the aerodynamics and heat transfer within the main gas path for partial and full stage turbines. Several rotating rig studies have also investigated rotor-stator cavity flows and rim seal performance to understand hot gas ingestion, where it is crucial to include rotational effects. These turbine research facilities have used one of two techniques to simulate engine representative conditions: (1) short duration flow, and (2) continuous duration flow. Continuous duration turbine rigs can be further separated into other categories, such as partially loaded, large scale, and true-scale fully loaded turbines.

Several short duration turbine rig facilities are reported in the literature including the following: Dunn and Stoddard [2] referred to hereafter as the Ohio State turbine rig (formerly at Calspan), Ainsworth et. al. [3] and Hilditch et. al. [4] referred

to hereafter as the Oxford turbine rig, Consigney et. al. [5] referred to as the VKI turbine rig, Haldeman et. al. [6] and Anthony et. al. [7] referred to as the AFRL turbine rig. Short duration rotating turbine facilities have provided important details regarding main gas path aerodynamics and heat transfer at engine-corrected conditions for full scale engine hardware. A few of these facilities are briefly summarized here. For a more detailed history of short-duration facilities the reader is referred to references [8-12].

The Ohio State turbine rig includes a combustor emulator upstream of the turbine, which allows for a wide variety of inlet temperature profiles to be tested. A separate blowdown circuit provides coolant. A typical test run results in 50 ms of data at steady conditions. The Oxford turbine rig is a short duration turbine research facility driven by a light isentropic piston tube capable of achieving steady conditions for 500 ms. The VKI turbine rig is a short duration facility driven by a piston tube capable of maintaining correct aerodynamic conditions for approximately 200 ms. Data are analyzed over a 30 ms time period, during which time the rig conditions, including rotor speed, are approximately steady state. The Turbine Research Facility at AFRL is a blowdown facility capable of test durations on the order of 2 seconds, and even longer for an extended duration test. A dual circuit cryogenic cooling system provides coolant flows to the inner and outer diameters of the engine test turbine. A combustor simulator also provides engine realistic pressure and temperature profiles entering the turbine.

Similar to the short duration facilities, there are many continuous duration flow turbine rigs in the open literature. The continuous duration flow rigs using partially-loaded turbines (not full stages) or large scale airfoils include those used by Roy et. al. [13, 14] referred to hereafter as ASU turbine rigs 1 and 2, Sangan et. al. [15] referred to as the Bath turbine rig, and Lakshminarayana et. al. [16] referred to as the Penn State low speed turbine rig. The continuous duration turbine rigs using true-scale fully loaded turbines include Gallier et. al. [17] referred to as the Purdue turbine rig, Sell et. al. [18] referred to as the ETHZ turbine rig, Bohn et. al. [19] referred to as the Aachen turbine rig, Schmitz [20] referred to as the Notre Dame turbine rig, Coren et. al. [21] referred to as the Sussex turbine rig, and Palafox et. al. [22] referred to as the GE turbine rig.

The ASU 1 turbine rig is a partial span turbine rig used to study hot gas ingestion in a rotor-stator cavity using partially loaded blades. The ASU 2 turbine rig examined a vane-blade configuration with higher vane exit swirl than the ASU 1 rig as well as reduced airfoil counts. The Bath rotating turbine rig operates at steady state with vanes and partially-loaded blades. The Bath rig has allowed for a detailed study of many rim seal geometries [23] with optical access for thermal measurements on both the stationary and rotating sides of the cavity [24]. The Penn State low speed turbine rig is a large scale, low speed, cold flow rotating turbine facility. The large scale allows for detailed spatial measurements in the main gas path similar to large scale wind tunnel cascades, with the inclusion of rotational effects providing important details regarding the main gas path.

Some of the true-scale, fully loaded, continuous flow turbine rigs are now briefly reviewed. The ETHZ turbine rig is a 2-stage axial turbine facility used to study the effects of unsteady flows on turbine aerodynamic performance. The facility is a closed-loop, continuous duration rig. The focus of the research is on the second stage turbine, which features an aerodynamically representative low pressure turbine under realistic operating conditions. The Notre Dame turbine rig is a closed-loop, steady state 1.5 stage low-pressure turbine research facility. The design includes a high-work and highly-loaded turbine (Φ=0.78, Zw=1.35) used to study main gas path aerodynamics and cooling purge flows. The Sussex turbine facility includes a two-stage continuous duration rig used to study inter-stage leakages and coolant delivery. Several coolant delivery modifications were designed into the rig allowing for systematic testing of the turbine stator cavity coolant flows. These experiments provided valuable validation data sets for further numerical studies [25, 26]. More recently, a GE turbine rig was commissioned to study rim seal geometries at relevant engine conditions. The rig is a continuous duration 1.5 stage turbine test facility that allows for modular rim seal designs on a bladed disk. Early experiments were used to validate reduced order computational design tools with good success [27].

Several continuous duration turbine facilities based on the open literature are shown in Figure 2 for both the United States and Europe [28]. Figure 2 shows the blade inlet Re_X versus the cavity rotational Re_ϕ. Most high pressure (HP) turbine disks within real gas turbine engines, especially intermediate and large size engines, experience $Re_\phi \geq 2 \times 10^7$ [29]. The graph shows that the operating envelope of most steady state rigs is still an order of magnitude lower in rotational Reynolds number than typical engine conditions.

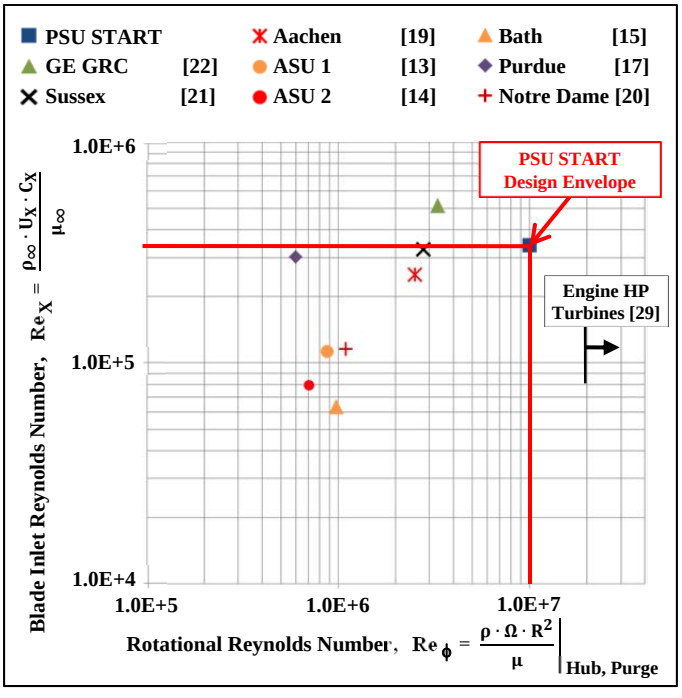

Figure 2. Design operating envelope of the Penn State START facility as compared to several continuous-duration, rotating turbine facilities [28].

There is a need in the open literature for engine relevant studies with rotation that focus beyond just the hot main gas path. More studies are needed that examine the systematic reduction in turbine cooling flows, the prevention of the hot main gas path from being ingested into the inner and outer cavities, better purge flow management, thermal protection of the disks, improvements in design of seals between adjacent stationary hardware and between rotor-stator gaps in hardware, and evaluating design improvements in airfoil and platform cooling features. The near term and long term phases of the PSU START facility provide the means to accomplish these studies and will provide critical engine relevant data to the current literature. The results and learning that will take place during the course of these studies will provide important validation of turbine engine design tools.

One of the goals for the PSU START facility is to push the operating rotational Reynolds number out to the same order of magnitude as most gas turbine engines while still maintaining the same blade inlet Reynolds number, allowing for unique test capabilities. The operating conditions for the new START rig are also shown in Figure 2, which more closely match that of most engine HP turbines. The remainder of this paper describes the development of the START facility, which is under construction and is expected to be operational in 2014.

FACILITY REQUIREMENTS

Simulating steady and unsteady interactions between the hot main gas path and the secondary air system at engine relevant scaling parameters translates into significant facility requirements. Continuous air flow supplies near 5.7 kg/s (12.5 lb_m/s) at 480 kPa (70 psia) were needed to accomplish this goal, with overall compressor power requirements above 1 Megawatt. Also needed was a considerable temperature difference between the main gas path at 395K (250°F) and the secondary air system at 275K (40°F). Furthermore, the new facility was designed to test a 1.5 stage rotating turbine with a disk speed of approximately 10,000 rpm and disk sizes between 0.4-0.6 m (16-24 inches) in diameter. These turbine disk operational speeds and sizes require a large turbine shaft brake and dynamometer system that can accurately control rotational speeds, which produce engine relevant ratios of axial to circumferential flow velocities.

Meeting all of the air flow, pressure, temperature, and power infrastructure requirements resulted in the design operating envelope for the new START facility, as was shown in Figure 2, being well above the current capability of most continuous duration, rotating turbine rigs in the U.S. and Europe. By reducing the temperature of secondary air system flow to well below the main gas path temperature, an increase in the rotational Reynolds number is achieved for a given rotational speed, disk size, and secondary air system supply pressure. It can be seen that the START operating envelope is within the same order of magnitude as a typical industrial gas turbine engine.

The facility and turbine design requirements mentioned above have been implemented for the near term Phase 1 operating capabilities of the START facility and are summarized in Table 1. The focus of Phase 1 testing is to study the influence of leakage flows from the internal secondary air system on turbine stage performance and efficiency by evaluating disruptive new designs in sealing interfaces between adjacent stationary components and between stationary and rotating components. Specifically, experiments focus on the inner diameter and inner cavity side of the secondary air supply system that includes the turbine disk and hub region of the airfoils, seals, and platforms. Therefore, the main gas path annulus was reduced to include span locations only from the hub to mid-span on the airfoils, resulting in half-span turbine vanes and blades. This approach has been successfully performed and reported in the literature by other researchers including Feiereisen [30] and Roy [13-14], and allowed the air flow capacity requirements to be cut approximately by half for Phase 1.

Table 1: Engine and START Turbine Conditions

Parameter at Blade Inlet	Aero-engine (cruise)	START Phase 1	START Phase 2
Coolant-to-Mainstream Density Ratio (ρ_∞/ρ_p)	2.0	1.3	2.0
Stage Pressure Ratio ($p_{o,in}/p_{0,ex}$)	2	1.5 - 2.5	1.5 – 2.5
Rotational Reynolds Number (Re_ϕ)	2.0E7+	<=1.0E7	<=2.0E7
Rotational Speed (rpm)	15000+	<= 11000	<= 13000
Mass flow rate (kg/s)	25+	5.7	11.4
Axial Reynolds Number (Re_x)	3.0E5	3.0E5	3.0E5
Blade Inlet Mach (Ma)	0.65	0.65	0.65
Airfoil Geometry	True Scale, Full Span	True scale, Half span	True Scale, Full Span

Current plans for the long term Phase 2 operation include doubling the air mass flow rate capability to near 11.4 kg/s (25 lbm/s) by adding a second identical large compressor, in parallel with the first compressor, that will allow studies to be performed using full span airfoils, larger turbine disk diameters, higher rotational speeds (higher Reϕ), and additional turbine stages. The facility electrical power infrastructure was designed and installed during Phase 1 to accommodate these long term Phase 2 operational goals requiring over 2 MW. This infrastructure included installing a new building 46kV power line and poles, a sub-station with transformer and metering cabinet, and a main 4160V switchgear room.

In addition to the planned increase in air flow capacity, potential Phase 2 considerations include adding a large heat addition process to significantly raise the temperature of the turbine main gas path flow to allow more realistic and accurate heat transfer experiments to be conducted. Other potential considerations for Phase 2 include introducing a profile generation device in the main gas path flow that would allow control over the radial and circumferential spatial profiles of air temperature and pressure entering the test turbine to investigate their influence on the performance of the turbine stage design being tested.

MECHANICAL DESIGN

The operation of the facility from a mechanical design flow path perspective is shown within the diagram in Figure 3. A large industrial compressor pulls approximately 5.2 m^3/s (11,000 SCFM) of air flow from outdoor atmospheric conditions of 100 kPa, 297K (14.5 psia, 75°F) on the facility roof, first through an inlet filter and weather hood and then into the compressor inlet. The two-stage centrifugal compressor with a 1.1 MW (1500 hp) motor then discharges the air flow at a nominal mass flow rate of 5.7 kg/s (12.5 lbm/s) at pressures up to 480 kPa (70 psia) at 395K (250°F). A series of controllable inlet guide vanes are located at the compressor inlet to allow flexibility in the compressor's operating curve of discharge pressure versus flow rate.

The large majority of the compressor discharge air flow is then directed through a large main pipe towards a settling chamber that is located upstream of the main test turbine. The settling chamber contains a series of baffles and screens to help ensure a uniform flow field enters the test turbine as the main gas path flow. After passing through the turbine, the flow is directed back towards the facility roof where it is exhausted to atmosphere through a silencer. Large venturi flow meters are used to measure the main gas path flow rate upstream of the turbine and downstream of the turbine.

A smaller secondary pipe, located just downstream of the compressor discharge, is used to extract up to approximately 20% of the compressor discharge flow and send it through thermal conditioning, moisture separation, and filtering processes in order to reduce the air flow temperature down to approximately 275K (40°F). This same cooled air flow is then directed to the turbine through four separate and independently controlled pipe lines, where the flow is strategically used as secondary turbine cooling, purge, and leakage air. Two of the four secondary air pipe lines supplies flow to the upstream side of the turbine disk, and similarly two to the downstream side of the turbine disk. The temperature reduction process establishes over 115 K (200°F) temperature difference between the turbine main gas path flow and the secondary air system flow. The flow rate passing through each of the four secondary air delivery pipe lines is measured using turbine flow meters with high turn down ratios.

The primary turbine shaft protrudes through the end of the turbine test section housing and is first flex-coupled to an inline, pedestal-mounted, torque meter that measures the turbine shaft torque. The torque meter is then flex-coupled to a water brake and dynamometer system that both measures and controls shaft rotational speed as well as provides a redundant measurement of shaft torque. The dynamometer system can continuously operate turbines up to a maximum of 0.9 MW (1200 hp) at speeds of 11,000 rpm.

The air flow pressure ratio across the turbine stage is maintained at the desired level using a large proportionally controlled valve located in the pipe downstream of the turbine. A by-pass system was also designed into the rig that allows some or all of the air flow to pass around the turbine test section during startup. In case of an emergency, two fast-acting (~ 0.5 sec) flow control valves were designed into the rig, one located in the by-pass system, and one located downstream of the turbine. The fast-acting valve located in

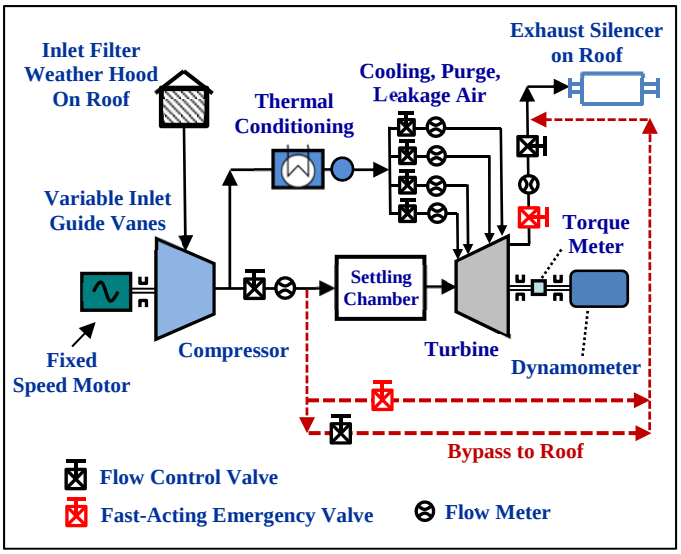

Figure 3. Mechanical flow path of the START facility showing the primary components of the rig.

the by-pass system is designed to be fully closed during normal operation, and will quickly open if an emergency shutdown sequence is executed, which will then direct the compressor discharge flow around the turbine test section and towards the facility roof exhaust. In contrast, the fast-acting valve located downstream of the turbine is designed to be fully open during normal operation, and will quickly close during an emergency to prevent any flow from passing through the turbine. Both emergency fast-acting valves serve to help mitigate high risk turbine operational scenarios, for example the prevention of a turbine shaft over-speed condition if the dynamometer were to experience temporary speed control problems, or if a shaft coupling were to loosen or break.

FACILITY LAYOUT

The new START facility is located within an existing Penn State research building near the main campus in State College, PA and consists of three primary rooms, shown in Figure 4, including a compressor room, test bay rig room, and a control room. The compressor room, shown in Figure 5, was sized to accommodate both Phase 1 and Phase 2 operational plans such that two compressors are installed onto their own isolated, three feet thick (0.9 m) concrete slabs (to eliminate vibration to and from the high speed rotating machinery). The air-end base frame of the two-stage compressor is field upgradeable such that it can include a third stage of compression to raise the discharge air pressure up to 1.1 MPa (165 psia) using a 1.9 MW (2500 hp) motor. Directly above the compressor room, a steel roof platform was installed that supports the large air intake and exhaust equipment systems.

The test turbine is located within the test bay room, which was sized to include the majority of the air flow pipe ductwork, settling chamber, turbine test section, secondary air system, water brake and dynamometer system, and an overhead crane system (5 ton capacity). The main components of the turbine test section are also positioned on an isolated thick concrete slab to eliminate any vibration to

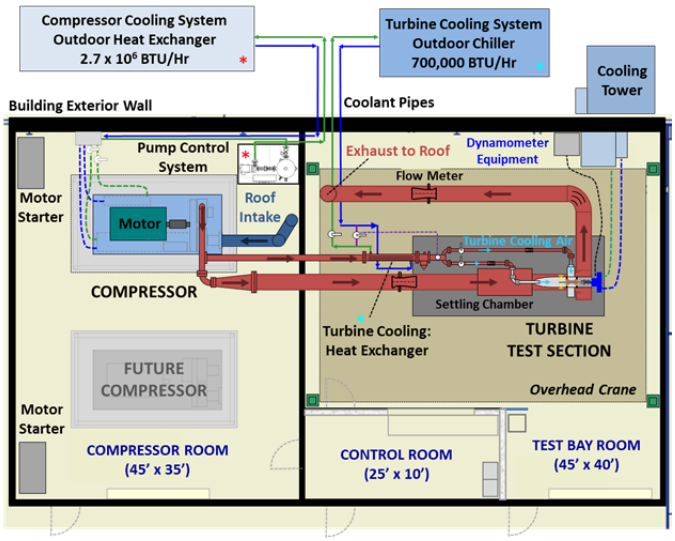

Figure 4. Schematic showing top view floor plan of the START facility.

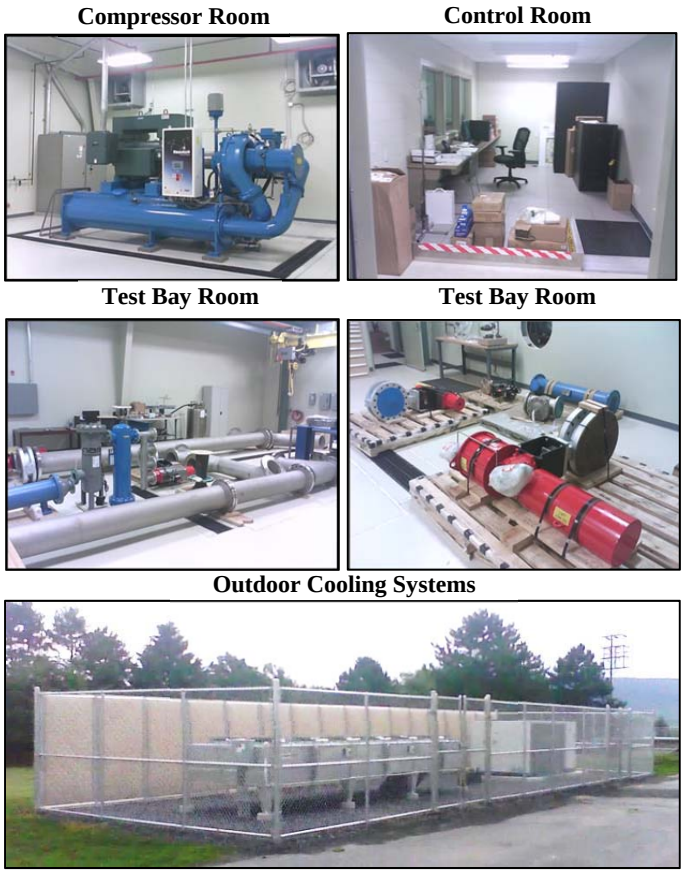

Figure 5. Photographs showing the main facility rooms and outdoor installations.

and from the high-speed turbine rotor system. An isolated control room was included adjacent to the turbine test section that includes the facility command center and data acquisition systems. The control room is constructed using 20.3 cm (8 inches) thick concrete walls, over 2.5 cm (1 inch) thick ballistic grade windows, and a raised floor system for easy routing of wires and cables.

Two large cooling systems were designed and installed for the facility. Both cooling systems include heat reject equipment located outdoors behind the facility, shown in Figure 5, which rejects the heat loads to atmosphere. The liquid coolant for both cooling systems is circulated to and from the outdoor equipment through separate 10 cm (four inch) diameter underground pipe systems that were designed for the cooling requirements of Phase 1 and Phase 2 operation.

One of the cooling systems is rated up to 800 kW (2.7 x 10^6 BTU/Hr) that removes heat generated within the compressor intercooler and oil cooler. This cooling system includes a pump and control skid located within the compressor room that circulates liquid coolant to and from the compressor and a large outdoor, forced-convection driven heat exchanger. The large fans on the heat exchanger are divided into stage groups that can be controlled to allow some flexibility in the compressor discharge air temperature.

The second cooling system is rated up to 200 kW (700,000 BTU/Hr) and includes an outdoor process chiller system that circulates liquid coolant to and from an in-line, shell-and-tube heat exchanger that is positioned in the test bay room within the air delivery pipe for the turbine secondary air system. A sensor is positioned downstream of the shell-and-tube heat exchanger to measure the air temperature of the turbine secondary air flow. This temperature sensor is used as an active input for a flow control valve that allows a portion of the liquid coolant to bypass the shell-and-tube heat exchanger, in order to maintain the turbine secondary air flow temperature at a steady user defined level. Phase 2 considerations include introducing liquid nitrogen based cooling in the secondary system heat exchanger to reduce air flow temperatures further below 275K (40°F).

FACILITY DUCTWORK

All of the air flow ductwork and valves located upstream and immediately downstream of the test turbine section, including the secondary air system piping, are made from stainless steel to eliminate the potential for rust formation and debris from entering the turbine. The pipe ductwork system, shown in Figure 6, ranges in size mostly from 20 cm (8 inch) through 40 cm (16 inch) diameter. Exhaust piping to the roof located downstream of the test turbine section in the vertical orientation is made from carbon steel and is painted with a high temperature primer and top coat. All of the pipe ductwork was designed to be capable of circulating the air flow at pressures up to 1.0 MPa (150 psig). In addition, certain sections of pipe were also designed for air flow temperatures up to 670K (1200°R), including the components upstream and downstream of the turbine test section, as well as the turbine test section itself.

The ductwork also includes other important components. A series of bellows expansion joints are installed at certain locations to allow for thermal expansion during operation, and most pipe sections are supported on steel beams with pipe rollers. Flange class ratings include 1.0 and 2.1 MPa (150 and 300 psig) sizes to account for the design pressure and temperatures. Just downstream of the compressor discharge,

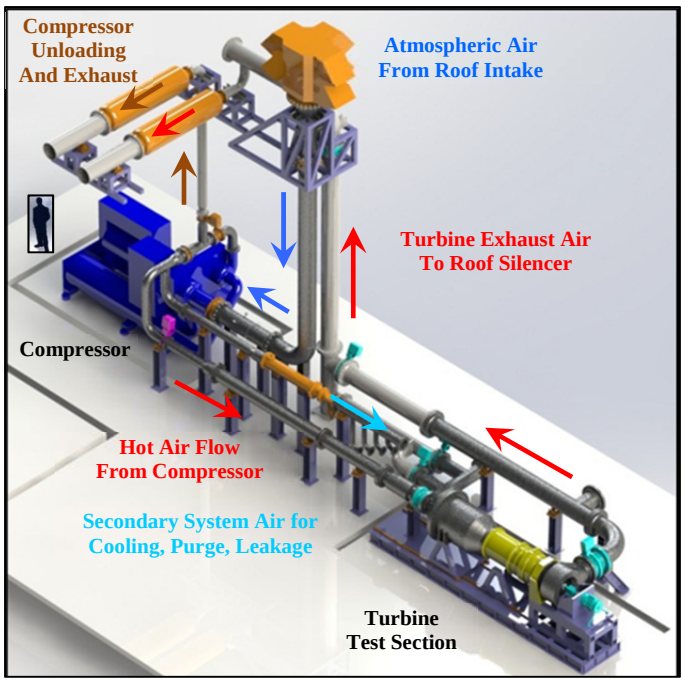

Figure 6. Drawing of the steel pipe ductwork system that delivers the main gas path flow and secondary flows to the turbine test section.

is a tee-branch, for which the pass-through air flow is directed towards the turbine test section, while the branch flow path leads to a separate isolated exhaust silencer on the roof platform. This branch flow pipe serves as a means to safely unload the compressor during the compressor startup and shutdown sequences. Immediately downstream of the tee - branch is a low pressure-loss check valve that prevents the air flow from reversing direction back towards the compressor discharge that could result in the machine to stall.

The secondary system air pipe flow first passes through a low pressure loss, shell-and-tube heat exchanger designed to reduce the temperature of 20% of the compressor discharge flow from 395K to 275K (250°F to 40°F). This same secondary air flow then passes through a centrifugal separator having a high 99% efficiency water moisture removal process over a wide air flow rate range from 25 - 125% of the separator design air flow rate. Finally, the secondary air flow then passes through a high capacity filtration process that removes particulates down to 0.01 micron with relatively low pressure loss. The cooled dry air then enters the turbine test section where it is used as cooling, purge, and leakage flows.

TEST SECTION AND ROTOR SYSTEM

The turbine test section, shown in Figure 7, consists of over one hundred individual stationary and rotating components. Multiple planes of separation were designed in both the axial and circumferential directions which serve to reduce time associated with hardware modifications and instrumentation changes. Most of the turbine test section from the upstream settling chamber to the main bearing block structure is mounted on cradles and a sliding rail system.

The upstream settling chamber contains a series of interchangeable baffles and screens to help mix out flow non-uniformities prior to the flow entering the turbine. This upstream chamber includes a series of airfoil struts that extend from the outer casing to the rig centerline that mechanically support a center-pipe section which extends axially from within the chamber, past the turbine, and to the bearing system. The center-tube body is used to route delivery hoses for the turbine secondary air system and instrumentation.

A relatively thick, dual outer casing wall was included in the vicinity of the 1.5 stage turbine airfoils and rotating disk to provide for a more easy transition from the Phase 1 half-span to the Phase 2 full-span airfoil testing, and also to provide adequate safety margin to fully contain a potential burst turbine disk. The design also includes two axial locations for installing turbulence grids upstream of the turbine.

The START turbine consists of a single solid shaft with an overhung turbine disk that is supported on magnetic bearings and operates in the sub-critical regime. Figure 8 shows a cross-section view of the rotor system with a generic geometry turbine. The magnetic bearing system includes one forward radial bearing and an aft combination radial and axial

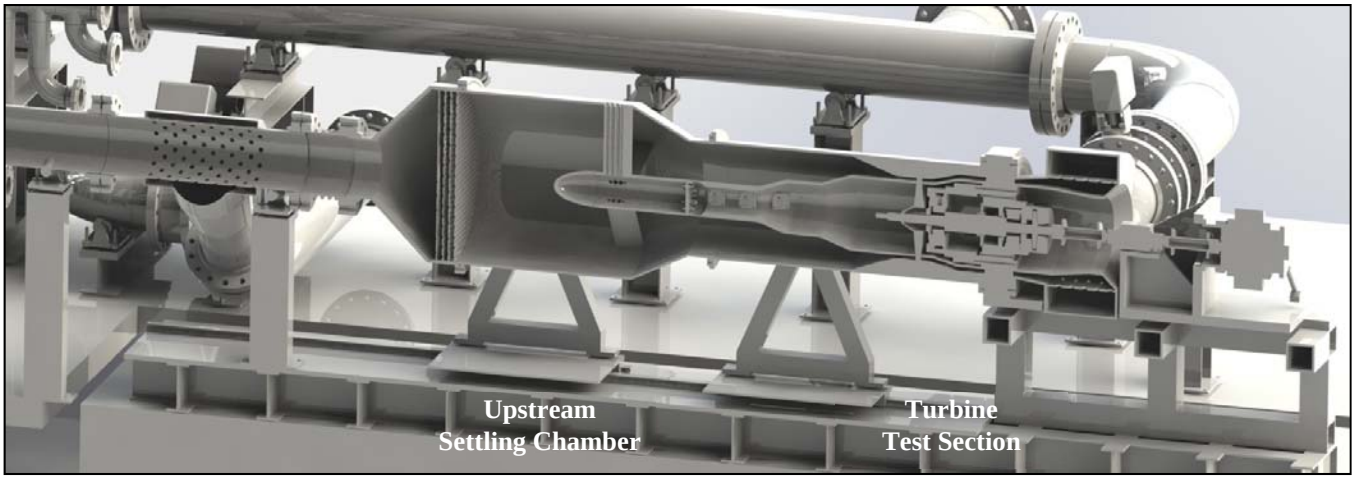

Figure 7. A solid model drawing with a cross-sectional view of the turbine test section (generic turbine shown).

supporting shaft rotational speeds up to 20,000 rpm. The forward radial bearing has a larger load capacity than the aft bearing to account for the additional radial load imposed by the overhung rotor. Auxiliary roller-element bearings are integrated into the magnetic bearing housings and are used mainly when the magnets are powered off, but are also used as emergency backup bearings.

The magnetic bearing system enables certain advantages over traditional rolling element and fluid based bearing systems. Magnetic bearings allow a controlled experiment in which the shaft centerline can be moved (offset) in both the axial and radial directions by 0.25-0.50 mm (0.010-0.020 inch scale) for accurate, continuous rotor placement and feedback, including shaft whirl orbits (non-circular). The electronic controller allows in-situ shaft and rotor system balancing and imbalance compensation, thereby eliminating the need for separate balance testing in separate machines. The magnetic bearing system can be tuned for any turbine system setup (within its radial and axial load capacity ranges) to achieve stable rotor system operation through the adjustment of bearing stiffness and damping. Additional benefits that the magnetic bearings offer include a no-loss torque measurement that improves measurement uncertainty, relatively quick setup, reduced wear and rig teardowns versus fluid bearings.

The magnetic bearing system selected also includes high frequency response (~15kHz) measurement sensors that accurately measure turbine shaft position and speed, as well as radial and axial loads. An emergency uninterruptable power supply is included to allow continuous and safe operation. Computer software for the electronic controller includes Ethernet access to allow the vendor to provide remote customized support and analysis of the system setup and operation.

Accurate axial placement of the rotating turbine hardware will also be accomplished (in addition to the magnetic bearings) using a series of precision gage spacer rings that are positioned onto the turbine shaft near the turbine disk arm spline and spanner nut. This controlled axial placement allows different gap sizes to be studied between stationary and rotating hardware.

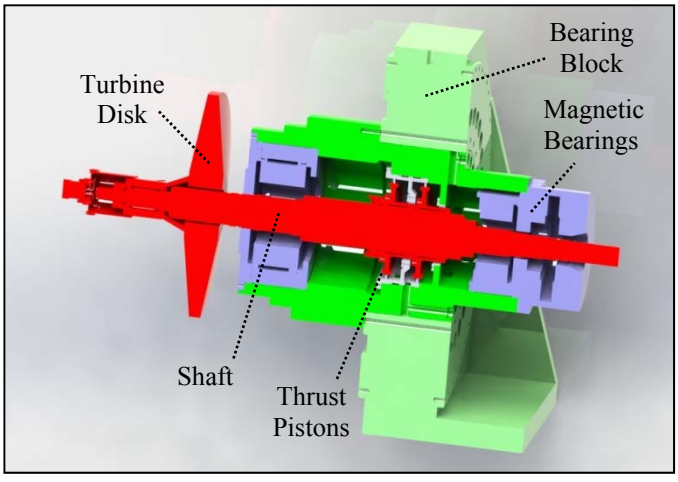

Figure 8. Solid model drawing showing the rotor and bearing system (generic turbine disk shown).

A tandem thrust piston arrangement is used to balance the axial load generated by the turbine disk. The pressure in each cavity, both upstream and downstream of the thrust pistons, is independently controlled by venting pressure regulators. Piston downstream pressures are set based on testing requirements (to control leakage), while the piston upstream pressure is controlled based on feedback from the magnetic bearing thrust load measurement. The supply air is provided by an auxiliary separate compressor. The outer diameter seal on the thrust piston is a commercially available brush seal, while the inner diameter uses a labyrinth seal.

A commercially available flexible coupling is used to connect the shaft to either a water brake dynamometer or a torque meter. A low moment and low mass configuration of the coupling was specified to improve rotor dynamic response. For initial tests, the shaft will be directly coupled to the water brake dynamometer; subsequent tests will be conducted with a high accuracy torque transducer that will be pedestal mounted between the turbine shaft and the dynamometer.

The rotor system rotor-dynamics was modeled using XLrotor [31]. Several assumptions were made to reduce modeling complexity based on the given maximum stiffness of the magnetic bearings including (1) the support housing and the dynamometer shaft were modeled with infinite stiffness and (2) the magnetic bearing is 15 or 35 times softer than the dynamometer or housing, respectively. The rotor dynamic model is shown in Figure 9. The fully assembled shaft weight is approximately 115 kg (250 lb) most of which is located on the forward radial bearing.

A Campbell diagram for the rotor dynamics of the shaft is shown in Figure 10. The natural frequencies of the rotor assembly are plotted as a function of rotor speed. The black dashed line represents a synchronous excitation, and the intersection of this line with a natural frequency shows a critical speed. The two low natural frequency modes are the rigid body modes, which are far from the design speed, and will be passed through quickly. The first bending mode does not cross the synchronous line until 14,800 rpm, which gives adequate margin over the design speed of 10,000 rpm. Several

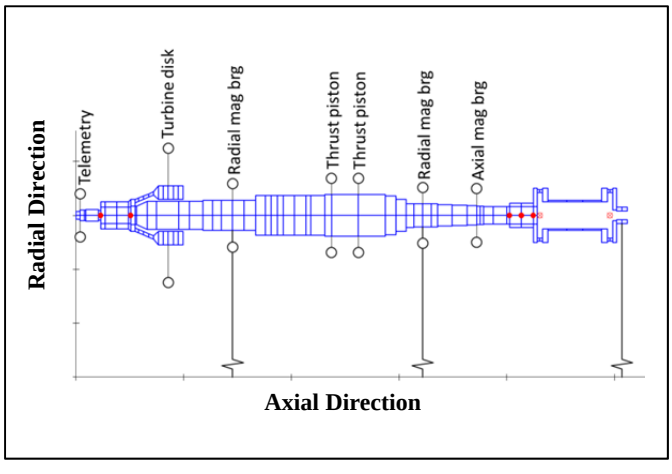

Figure 9. Diagram showing the model used for rotor dynamics.

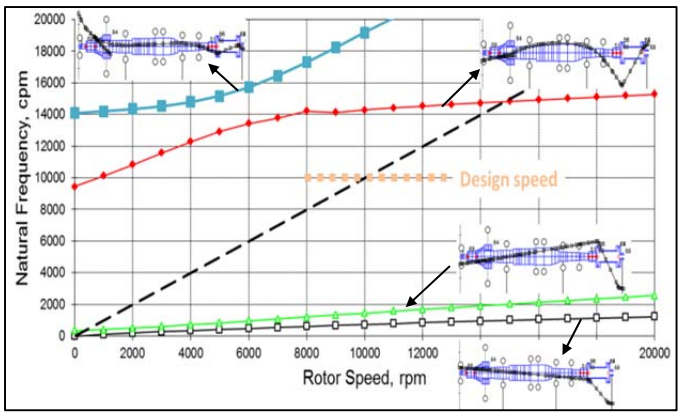

Figure 10. Campbell diagram of the rotor dynamics analysis showing adequate margins.

iterations of shaft design were required to achieve this adequate margin. The stability analysis of the rotor system is being performed by the magnetic bearing vendor using proprietary software.

CONTROL AND SAFETY

A programmable logic control (PLC) system for the facility and rig was designed and integrated, as shown in Figure 11, to receive compressor conditions, turbine conditions, and other equipment and instrumentation signals all to allow safe, balanced turbine testing. The facility is designed to operate in an automated mode but does contain certain manual overrides. Process and instrumentation diagrams were first developed, followed by the design and integration of the hardware and software. The software and hardware are flexible by design to allow future expansion to be included with relative ease. The PLC system includes a visual display computer program with touch buttons to fully interact with the rig during start-up, testing, and shut-down.

Acceptable ranges of turbine pressure ratio, speed, and torque are incorporated into the PLC system. Acceptable ranges of the various equipment signals are also designed into the PLC system including the compressor, cooling systems, flow valves, magnetic bearing system, dynamometer, as well as stand-alone instrumentation. Interlocks and inputs from the data acquisition system provide instructions for continuous operation versus shutdown procedures involving commanding the dynamometer to brake, unloading the compressor, and by-passing air flow around the turbine test section. Moving between individual turbine operating points during testing is possible without having to go through a full shutdown sequence since experiment control is through both the high speed data acquisition system as well as the PLC. Both the PLC system and data acquisition system monitor the entire facility and rig operation at data rates consistent with high risk failure scenarios including turbine over-speed and over-pressure. Additional facility safety designs not already mentioned include a steel laboratory safety shield that surrounds the turbine test section.

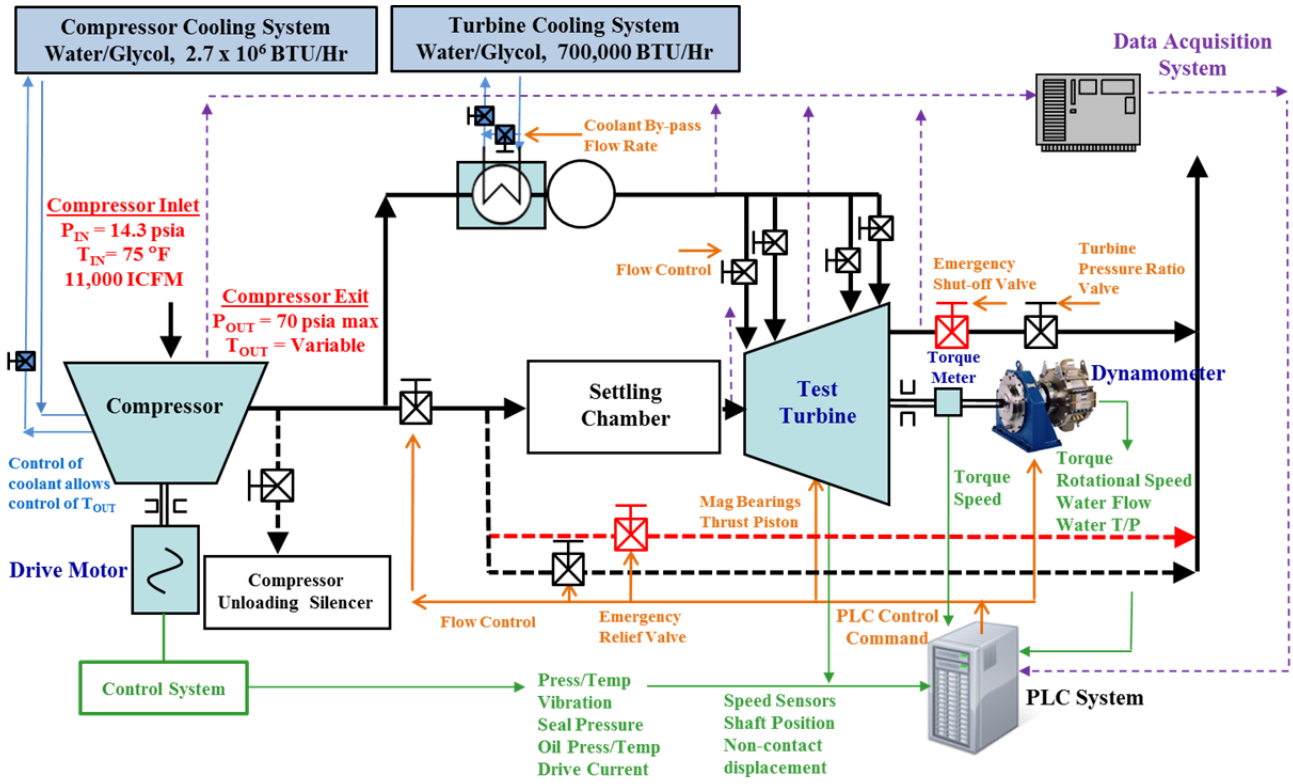

Figure 11. Diagram of the PLC system interactions with main equipment, sensors, and data acquisition.

INSTRUMENTATION

An instrumentation plan for the entire facility, rig, and turbine test section was developed to investigate the many governing aerodynamic and heat transfer parameters and variables related to turbine performance. The instrumentation plan was structured around obtaining some of the most accurate measurements conducted in the field of gas turbine research using engine scale hardware. The plan includes a wide variety of sensors at many locations within the turbine test section, as shown in Figure 12, including surface and air flow temperatures, surface and air flow pressures, as well as hardware proximity clearance probes. Considering the spatial constraints of the true scale engine hardware, the instrumentation type, construction, placement, and routing path for each sensor were carefully selected and designed.

The instrumentation design allows for measurements of the flow and thermal field pressure, velocity, and temperature at the first vane inlet and exit as well as at the second vane inlet and exit using both radial and circumferential traverses. These traverses also allow measurement of flow angles using multi-headed pressure probes, and turbulence intensity using hotwire anemometry. The turbine stage total-to-total adiabatic efficiency will be determined using these measurements.

The first and second stage vanes were designed to allow instrumentation wires and tubes to be internally routed within the vanes from the inner diameter cavity side to the outside of the rig. The vanes were constructed using an additive manufacturing technique involving a metal laser sintering process. This process constructs the vanes by melting very thin layers (20 μm) of powdered metal, one layer at a time, such that instrumentation can be incorporated directly into the vane as the part is "grown". This instrumentation included several small static-pressure hole taps in the airfoil external wall surface, and hollow tubes within the airfoil solid. The static-pressure holes were included from the leading edge to the trailing edge on both the airfoil suction and pressure surfaces at three vane span height locations on multiple vanes to determine airfoil loading. Figure 13 shows an example generic airfoil that was designed and constructed to investigate the accuracy of the additive manufacturing process from multiple vendors.

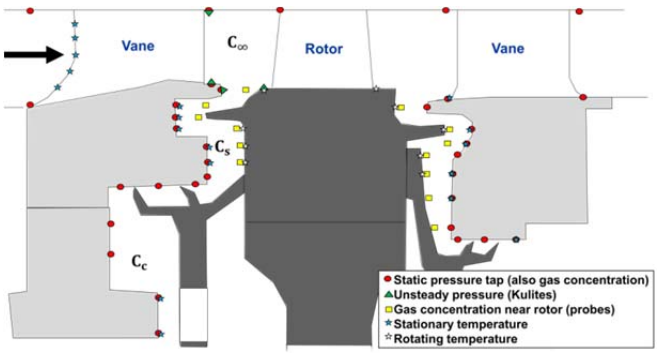

Figure 12. Schematic cross-section of the turbine showing main gas path and cavity instrumentation.

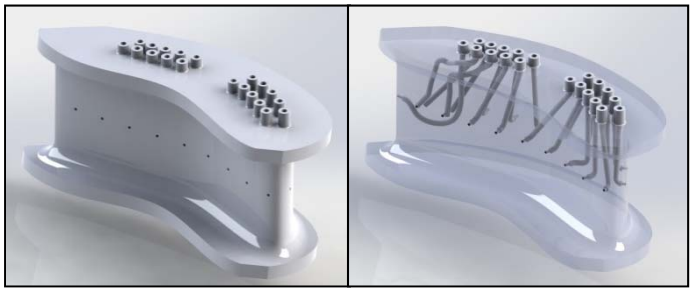

Figure 13. Illustrations showing example parts that were constructed using additive manufacturing that included instrumentation within the airfoils.

An intelligent pressure scanner system (approximately 100 channel capacity, 0.05% full scale accuracy, including multiple pressure ranges) is used to survey several hundred static pressure taps located within the turbine test section at a variety of locations in the main gas path, the front rim seal and cavity, and in the aft rim seal and cavity. Static pressure taps are also located at several radial and circumferential locations on the stationary hardware, as shown in Figure 12, in the front and aft cavities to accurately map out the secondary flow boundary conditions for reduced order model validation.

Circumferential variations due to the gas path vane-blade interactions are attenuated deeper in the cavity, therefore higher tap quantities are located closer to the main gas path. Unsteady pressure is measured using a series of Kulite pressure transducers in the first vane and blade gap, and in the front cavity. Ultra-miniature cylindrical pressure transducers and thin surface mount pressure transducers are placed on both stationary and rotating hardware to characterize the vane-blade unsteady interactions that affect rim seal ingestion.

The strategically placed static pressure taps along the vane endwalls and within the static walls of the rim seal cavity region will also be used to spatially track CO_2 tracer gas that is injected into the turbine cooling and leakage flows. The tracer gas is used to monitor the ingress and egress behavior patterns of the turbine cooling and leakage flow to and from the inner diameter cavity region. A high accuracy gas analyzer and sampler is connected directly to the measurement taps. In addition, probes allow for gas concentration measurements close to the rotor. The gas samples are continuously flowed to a Siemens Ultramat 6E gas analyzer, which uses a narrow-band infrared absorption technique to determine CO_2 concentration. The analyzer has negligible zero drift, and due to the measurement technique, it is not affected by humidity in the measurements, which can be a problem for IR gas analyzers. Benchmarking experiments have shown <2% uncertainty over a wide range of sealing effectiveness values.

The turbine test section hardware has been designed to accommodate both a telemetry system and a slip-ring system connected to the fore end of the turbine shaft for rotating instrumentation mounted on the blades, disk, cover plates, and seals. Initial testing during Phase 1 includes a telemetry system that is configurable for between 10-21 channels depending on the transmitter type used. The 10 channel static transmitter has a frequency response from DC to approximately 20 kHz and can be configured for any

combination of strain gages, pressure transducers, thermocouples, and RTD's. The 21 channel dynamic transmitter has a frequency response from 10 Hz - 38 kHz that is configurable to include 10 channels of strain and pressure, 10 channels of thermocouples, and an RTD.

Blade tip clearance is measured at various circumferential locations with capacitance probes, which have a high displacement to sensor diameter ratio. The signals from the capacitance probes are handled by an amplification and processing system. A high frequency processor is needed to determine the blade tip clearance, otherwise the peak could be missed and there could be a time lag [32]. The system receives the high frequency signal produced by the passing blades (up to 5 MHz) and reduces the data to an analog signal proportional to the blade tip clearance, which is then read in by the data acquisition system at a reduced speed. This allows for real-time tip clearance measurements with 1-2% accuracy of the tip clearance measurement.

Measurement of turbine shaft rotational speed and torque will be used to determine torque-based efficiency, rotational Reynolds numbers, and stage power. Both the dynamometer system and torque transducer allow accurate measurements of both. The dynamometer was initially fitted with a lower range torque load cell between 0-500 Nm (0-375 ft-lbf) in order to increase measurement accuracy. A 0.2% full scale torque accuracy on the load cell is standard combined with a 0.1% full scale torque accuracy on the full range torque of 0-1200 Nm (0-900 ft-lbf). To complement these measurements, the pedestal mounted torque meter has an increased accuracy of 0.1% over the same range of operating conditions.

PLANNED TEST CAMPAIGNS

A series of initial test campaigns were developed to first examine how turbine stage efficiency can be further increased by implementing better sealing technologies that prevent the critical inner- and inter-stage leakage problems addressed in studies such as [33, 34]. Phase 1 testing using the arrangement shown on the left of Figure 14, will focus on reducing secondary air system leakage by examining the effectiveness of different designs of rotor-stator rim seals. Testing will first involve evaluating the 1.5 stage turbine to establish baseline performance maps without secondary air system cooling flow.

The baseline qualification data will include characterizing the turbine stage pressure loss, efficiency, and airfoil loading. Spatially resolved temperature and pressure field surveys will be conducted at the inlet of the first stage vane, exit of the first stage vane (blade inlet), exit of the first stage blade, and exit of the second stage vane. Airfoil pressure loading will be measured at multiple span height locations and circumferential locations. Main gas path flow characterization will also be performed by evaluating circumferential and radial flow uniformity, the turbine stage axial and rotational Reynolds numbers as well as turbulence intensity and length scale. Turbine stage design validation will also be analyzed by collecting data relevant to stage loading including Zweifel coefficient, axial flow coefficient, and reaction.

Following the initial baseline testing, the 1.5 stage turbine performance will be evaluated again but with secondary air system cooling flow and an initial design for the sealing hardware. The individual secondary cooling flows will be varied, along with the disk rotational speed and gap size between stationary and rotating components. The results will then be aligned with pre-test predictions, and will be used to develop an improved design of the sealing hardware features. The enhanced hardware design will then be evaluated by performing a similar performance mapping of the 1.5 stage turbine over a range of operating conditions.

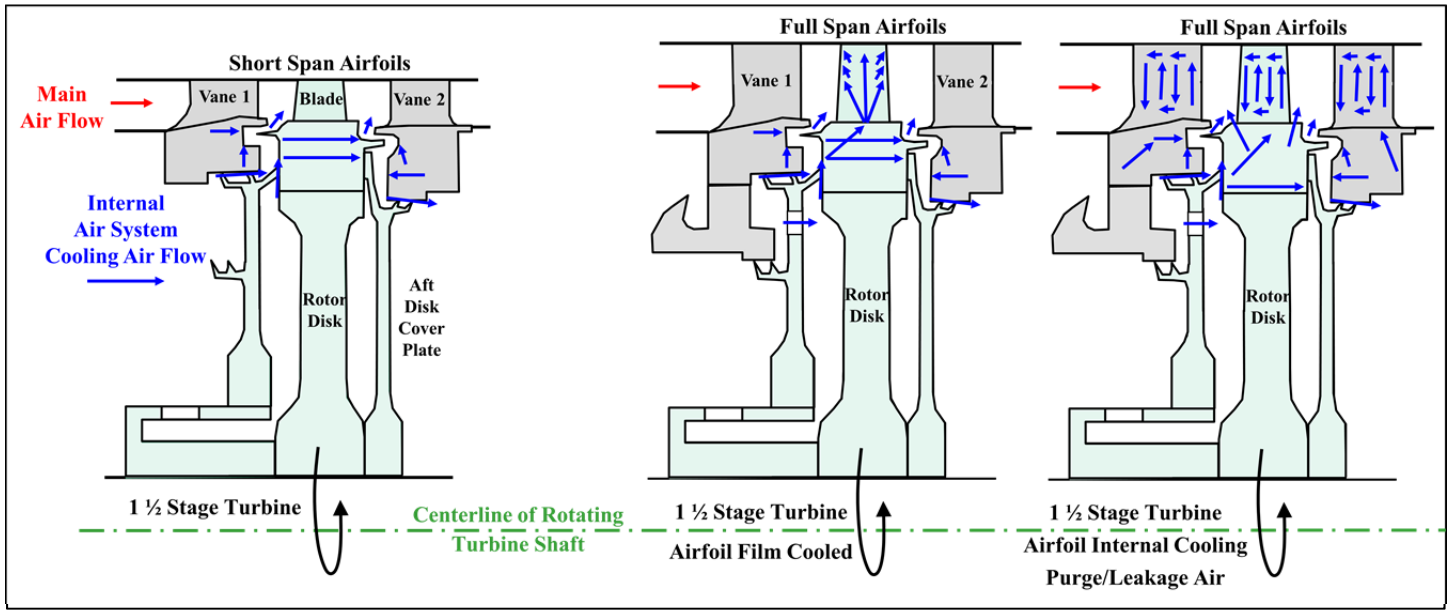

Figure 14. Schematic cross-section of the 1.5 stage test turbine arrangements that will be used to evaluate and develop improved turbine sealing and cooling designs.

Phase 2 testing, using the arrangement on the right of Figure 14, will focus on heat transfer including stage airfoils, platforms, cavities, and disks, all with leakage flow interactions using full span airfoils. Testing will again first involve evaluating the 1.5 stage turbine design to establish baseline performance maps without secondary air system cooling flow. Following this initial baseline testing, the 1.5 stage turbine design will be evaluated again but with the secondary air system flows including internal airfoil cooling. The individual secondary cooling flows will be varied, along with the disk rotational speed and gap size between stationary and rotating components. The results will then again be aligned with pre-test predictions, and will be used to develop an improved design of the cooling and sealing hardware features. The enhanced hardware design will then be evaluated by performing a similar performance mapping of the 1.5 stage turbine over a range of operating conditions.

Long term testing will focus on 1.5 stage turbine performance optimization by combining best designs of Phase 1 and Phase 2. Beyond the initial Phase 1 and Phase 2 test plans, this new START facility allows a wide range of sealing and cooling investigations to be performed at various points within the turbine stage including mate-face gaps, platforms, disk cover plates, and shaft seals. This new facility also allows engine manufacturers to test their true-scale hardware at engine realistic scaling parameters in order to significantly reduce the turbine development time and cost. The engine hardware designs can be tested over a range of operating conditions to investigate performance related to cycle variations.

CONCLUSION

A new world-class gas turbine research facility was designed and is currently being constructed that will allow engine-representative rotating turbine hardware to be tested in a continuous, steady-state, high-pressure flow environment. The new START facility includes a 1.5 stage turbine that simulates the aerodynamic flow and thermal field interactions in the engine between the hot mainstream gas path and the secondary air flows at relevant corrected operating conditions and scaling parameters.

The uniqueness of this facility includes a continuous duration facility with engine-relevant rotational and axial Reynolds and Mach numbers at the blade inlet. The design operating envelope for the new START facility is above the current capability of most continuous duration, rotating turbine rigs in the U.S. and Europe reported in the open literature and was designed to be within the same order of magnitude as a typical turbine engine. In addition, a magnetic bearing system is used to provide continuous accurate rotor feedback, micro-positioning of the turbine shaft, a no-loss torque measurement, and in-situ balancing.

The new facility and rig are also a platform for cost effective technology development and testing. Testing in the new facility is planned to begin in 2014 and will take place in two phases. The first phase is focused on understanding the behavior of inner-stage gap flow leakages in the presence of the main gas path and the rotating blade platform. The second phase is focused on developing and testing novel cooling methods for turbine airfoils, platforms, and disks, ultimately leading to an integrated approach for more effective use of the secondary cooling flow.

Most of the results from testing will be available for publication in non-dimensional form. The new facility will promote collaborative interactions between academia, government agencies, and industry to advance the development of gas turbine sealing and cooling technology, and will provide a vehicle for visiting researchers and training of our nation's future scientists and engineers.

ACKNOWLEDGEMENTS

The authors would like to recognize and thank Pratt & Whitney and the U.S. Department of Energy N.E.T.L. for their support. Efforts were performed under U.S. Department of Energy N.E.T.L. Contract DE-FE-0004000.3.622.053.001.

REFERENCES

[1] Internet websites www.pwps.com for PW Power Systems (a group company of Mitsubishi Heavy Industries, LTD.) and www.pw.utc.com for Pratt & Whitney (a United Technologies Company).

[2] Dunn, M. G., and Stoddard, F. J., "Application of Shock-Tube Technology to the Measurement of Heat-Transfer Rate to Gas Turbine Components," Proceedings of the 11th International Symposium on Shock Tubes and Waves.

[3] Ainsworth, R. W., Schultz, D. L., Davies, M. R. D., Forth, C. J. P., Hilditch, M. A., and Oldfield, M. L. G., 1988, "A Transient Flow Facility for the Study of the Thermofluid-Dynamics of a Full State Turbine under Engine Representative Conditions," ASME Paper No. 88-GT-144.

[4] Hilditch, M. A., Fowler, A., Jones, T. V., Chana, K. S., Oldfield, M. L. G., Ainsworth, R. W., Hogg, S. I., Anderson, S. J., and Smith, G. C., 1994, "Installation of a Turbine Stage in the Pyestock Isentropic Light Piston Facility," ASME Paper No. 94-GT-277.

[5] Consigney, H., and Richards, B. E., 1982, "Short Duration Measurements of Heat Transfer Rate to a Gas Turbine Rotor Blade," ASME J. Eng. Power, **104**(3), pp. 542-550.

[6] Haldeman, C. W., Dunn, M. G., MacArthur, C. D., and Murawski, C. G., 1992, "The USAF Advanced Turbine Aerothermal Research Rig (ATARR)," AGARD CP-319.

[7] Anthony, R. J., Clark, J. P., Finnegan, J. M., and Johnson, D., 2012, "Modifications and Upgrades to the AFRL Turbine Research Facility," ASME Paper No. GT2012-70084.

[8] Dunn, M., and Mathison, R., 2013, "History of Short-Duration Measurement Programs Related to Gas Turbine Heat Transfer, Aerodynamics, and Aeroperformance at Calspan and OSU," ASME Paper No. GT2013-94926.

[9] Chana, K., Cardwell, D., and Jones, T., 2013, "A Review of the Oxford Turbine Research Facility," ASME Paper No. GT2013-95687.

[10] Anthony, R. J., and Clark, J. P., 2013, "A Review of the AFRL Turbine Research Facility," ASME Paper No. GT2013-94741.

[11] Paniagua, G., Sieverding, C. H., and Arts, T., 2013, "Review of the Von Karman Institute Compression Tube Facility for Turbine Research," ASME Paper No. GT2013-95984.

[12] Epstein, A., Guenette, G., and Norton, R. J. G, 1984, "The MIT Blowdown Turbine Facility," ASME Paper No. 84-GT-116.

[13] Roy, R. P., Xu, G., Feng, J., and Kang, S., 2001, "Pressure Field and Main-Stream Gas Ingestion in a Rotor-Stator Disk Cavity," ASME Paper No. 2001-GT-0564.

[14] Roy, R. P., Feng, J., Narzary, D., Saurabh, P., and Paolillo, R. E., 2004, "Experiments on Gas Ingestion through Axial-Flow Turbine Rim Seals," ASME Paper No. GT2004-53394.

[15] Sangan, C. M., Pountney, O. J., Zhou, K., Wilson, M., Owen, J. M., and Lock, G. D., 2011, "Experimental Measurements of Ingestion through Turbine Rim Seals. Part 1: Externally-Induced Ingress," ASME Paper No. GT2011-45310.

[16] Lakshminarayana, B., Camci, C., Halliwell, I., and Zaccaria, M., 1996, "Design and Development of a Turbine Research Facility to Study Rotor-Stator Interaction Effects," Int. J. of Turbo and Jet Engines (**13**), pp. 155-172.

[17] Gallier, K. D., Lawless, P. B., and Fleeter, S., 2000, "Investigation of Seal Purge Flow Effects on the Hub Flow Field in a Turbine Stage using Particle Image Velocimetry," AIAA Paper No. AIAA-2000-3370.

[18] Sell, M., Schlienger, J., Pfau, A., Treiber, M., and Abhari, R. S., 2001, "The 2-Stage Axial Turbine Test Facility 'LISA'," ASME Paper No. 2001-GT-0492.

[19] Bohn, D. E., Decker, A., Ma, H., and Wolff, M., 2003, "Influence of Sealing Air Mass Flow on the Velocity Distribution In and Inside the Rim Seal of the Upstream Cavity of a 1.5-Stage Turbine," ASME Paper No. GT2003-38459.

[20] Schmitz, J. T., 2010, "Experimental Measurements in a Highly Loaded Low Pressure Turbine Stage," PhD thesis, University of Notre Dame, Indiana.

[21] Coren, D. D., Atkins, N. R., Turner, J. R., Eastwood, D. E., Davies, S., Childs, P. R. N., Dixon, J., and Scanlon, T. S., 2010, "An Advanced Multi-Configuration Stator Well Cooling Test Facility," ASME Paper No. GT2010-23450.

[22] Palafox, P., Ding, Z., Bailey, J., Vanduser, T., Kirtley, K., Moore, K., and Chupp, R., 2013, "A New 1.5 Stage Turbine Wheelspace Hot Gas Ingestion Rig (HGIR) – Part I: Experimentatl Test Vehicle, Measurement Capability and Baseline Results," ASME Paper No. GT2013-96020.

[23] Sangan, C. M., Pountney, O. J., Scobie, J. A. Wilson, M., Owen, J. M., and Lock, G. D., 2012, "Experimental Measurements of Ingestion through Turbine Rim Seals. Part 3: Single and Double Seals," ASME Paper No. GT2012-68493.

[24] Pountney, O. J., Sangan, C. M., Lock, G. D., and Owen, J. M., 2012, "Effect of Ingestion on Temperature of Turbine Discs," ASME Paper No. GT2012-68496.

[25] Coren, D. D., Atkins, N. R., Long, C. A., Eastwood, D., Childs, P. R. N., Guijarro-Valencix, A., and Dixon, J. R., 2011, "The Influence of Turbine Stator Well Coolant Flow Rate and Passage Configuration on Cooling Effectiveness," ASME Paper No. GT2011-46448.

[26] Dixon, J. A., Guijarro-Valencia, A., Coren, D., Eastwood, D., and Long, C., 2012, "Main Annulus Gas Path Interactions – Turbine Stator Well Heat Transfer," ASME Paper No. GE2012-68588.

[27] Ding, Z. Palafox, P., Moore, K., Chupp, R., and Kirtley, K., 2013, "A New 1.5 Stage Turbine Wheelspace Hot Gas Ingestion Rig (HGIR) – Part II: CFD Modeling and Validation," ASME Paper No. GT2013-96021.

[28] Thole, K., Barringer, M., and Alvin, M. A., 2011, "Development of a Rotating Rig to Study Secondary Flow Leakages and Aerothermal Cooling," DOE-NETL RUA FY11 Q1 Stakeholder's Review, January 11, 2011.

[29] Childs, P. R. N., 2011, Rotating Flow, Butterworth-Heinemann, Elsevier, Oxford.

[30] Feiereisen, J. M., Paolillo, R. E., and Wagner, J., 2000, "UTRC Turbine Rim Seal Ingestion and Platform Cooling Experiments," AIAA Paper No. AIAA-2000-3371.

[31] Murphy, B.T., 2012, "XLRotor Version 3.91", Austin, Texas. http://www.xlrotor.com/

[32] Haase, W. C., and Haase, Z. S., 2013, "High-Speed, Capacitance-Based Tip Clearance Sensing," IEE Aerospace Conference, Paper 2183.

[33] Wang, C.Z., Johnson, B.V., Mathiyalagan, S.P., Glahn, J.A., and Cloud, D.F., 2012, "Rim Seal Ingestion in a Turbine Stage from 360-Degree Time-Dependent Numerical Simulations," ASME Paper GT2012-68193.

[34] Mirzamoghadam, A.V., Giebert, D., Molla-Hosseini, K., and Bedrosyan, L. "The Influence of HPT Forward Disc Cavity Platform Axial Overlap Geometry on Mainstream Ingestion," ASME Paper No. GT2012-68429.